Different Hormonal Regulation of Cellular Differentiation and Function in Nucellar Projection and Endosperm Transfer Cells: A Microdissection-Based Transcriptome Study of Young Barley Grains[1][W]

Johannes Thiel*, Diana Weier, Nese Sreenivasulu, Marc Strickert, Nicola Weichert, Michael Melzer, Tobias Czauderna, Ulrich Wobus, Hans Weber, and Winfriede Weschke

Leibniz-Institut für Pflanzengenetik und Kulturpflanzenforschung, D–06466 Gatersleben, Germany

Nucellar projection (NP) and endosperm transfer cells (ETC) are essential tissues in growing barley (*Hordeum vulgare*) grains, responsible for nutrient transfer from maternal to filial tissues, endosperm/embryo nutrition, and grain development. A laser microdissection pressure catapulting-based transcriptome analysis was established to study NP and ETC separately using a barley 12K macroarray. A major challenge was to isolate high-quality mRNA from preembedded, fixed tissue while maintaining tissue integrity. We show that probes generated from fixed and embedded tissue sections represent largely the transcriptome (>70%) of nonchemically treated and nonamplified references. In NP, the top-down gradient of cellular differentiation is reflected by the expression of C3HC4-type ubiquitin ligases and different histone genes, cell wall biosynthesis and expansin/extensin genes, as well as genes involved in programmed cell death-related proteolysis coupled to nitrogen remobilization, indicating distinct areas simultaneously undergoing mitosis, cell elongation, and disintegration. Activated gene expression related to gibberellin synthesis and function suggests a regulatory role for gibberellins in establishment of the differentiation gradient. Up-regulation of plasmalemma-intrinsic protein and tonoplast-intrinsic protein genes indicates involvement in nutrient transfer and/or unloading. In ETC, AP2/EREBP-like transcription factors and ethylene functions are transcriptionally activated, a response possibly coupled to activated defense mechanisms. Transcriptional activation of nucleotide sugar metabolism may be attributed to ascorbate synthesis and/or cell wall biosynthesis. These processes are potentially controlled by trehalose-6-P synthase/phosphatase, as suggested by expression of their respective genes. Up-regulation of amino acid permeases in ETC indicates important roles in active nutrient uptake from the apoplastic space into the endosperm.

Developing seeds are sink tissues depending on nutrient supply from vegetative tissues. Nucellar projection (NP) and endosperm transfer cells (ETC) are responsible for nutrient transfer from maternal to filial tissues and, as such, represent nourishing tissues with an important role for endosperm growth and development. During grain development, the differentiation and function of NP and ETC have to be coordinated with changing sink strength. The NP differentiates from nucellus tissue facing the main vascular bundle. The organ shows a complex pattern of simultaneous cell division, differentiation, and disintegration to ensure nutrient supply in a regulated manner. It has been shown that release of nutrients from the nucellus and NP is partially associated with programmed cell death (PCD; Radchuk et al., 2006).

Likewise, endosperm formation is highly regulated. Within the syncytium, the cytoplasmic formation of phragmoplasts and inward-directed cell growth coincide with periclinal cell divisions forming the first endospermal cell layer. During further growth, peripheral cell layers show anticlinal cell division different from that of the starchy endosperm, which enlarges by periclinal cell division (Olsen, 2001). Anticlinal cell division positions all daughter cells in the same surface, thereby ensuring surface growth in relation to endosperm expansion (Olsen, 2007) and determining cell identity in the protoderm as an independent cell lineage (Laux and Jürgens, 1997). Differentiation of ETC and aleurone cell layers starts during the syncytial stage adjacent to NP (Olsen, 2004). ETC becomes functional around 6 d after flowering (DAF; Weschke et al., 2000). Within the endosperm, ETC and aleurone cells are the only persisting tissues, whereas starchy endosperm cells undergo PCD. ETC develop cell wall ingrowths to increase transport-active surfaces in accordance with their role in nourishment and solute supply (Thompson et al., 2001; Borisjuk et al., 2002; Offler et al., 2002). Despite our knowledge about solute transfer from maternal to filial grain tissues (Patrick and Offler, 2001; Zhang et al., 2007) and the morphology of NP and ETC (Patrick and Offler, 1995; Weschke et al., 2000; Radchuk et al., 2006), little is known about

[1] This work was supported by the Deutsche Forschungsgemeinschaft (grant no. 39205123) and the Federal Ministry of Education and Research (grant no. 0313821A).

* Corresponding author; e-mail thielj@ipk-gatersleben.de.

The author responsible for distribution of materials integral to the findings presented in this article in accordance with the policy described in the Instructions for Authors (www.plantphysiol.org) is: Johannes Thiel (thielj@ipk-gatersleben.de).

[W] The online version of this article contains Web-only data.

www.plantphysiol.org/cgi/doi/10.1104/pp.108.127001

specific gene expression patterns in these important organs.

Recent expression profiling experiments to study barley (*Hordeum vulgare*) grain development used manual dissection to separate maternal pericarp and filial endosperm and embryo fractions (Sreenivasulu et al., 2004, 2006, 2008). Because dissection boundaries are predetermined by the presence and position of dynamic cell layers, the interpretation of expression profiles is critical due to problems in precisely allocating distinct tissue types. Moreover, specific tissues or cell layers inside the caryopsis are not accessible by manual dissection. To overcome these limitations, laser capture microdissection and microdissection coupled with laser pressure catapulting (LMPC) have been developed. Combinations with large-scale gene expression analysis have been frequently used for mammalian systems (Emmert-Buck et al., 1996; Luo et al., 1999; Burgemeister et al., 2003). In plants, such applications have been used to monitor gene expression in maize (*Zea mays*) epidermis, vascular tissues, roots, and shoot apical meristem (Nakazano et al., 2003; Woll et al., 2005; Ohtsu et al., 2007) and Arabidopsis (*Arabidopsis thaliana*) embryo cells (Casson et al., 2005; Spencer et al., 2006) and siliques (Cai and Lashbrook, 2006). Developing barley caryopses contain cell types largely differing in structure, such as the cells within the degenerating maternal and differentiating filial tissues, which complicates the preservation of morphology during fixation and embedding. In addition, RNA extraction from the hard and rigid starchy endosperm during later maturation as well as from fixed and embedded material requires specific procedures.

We adapted LMPC-coupled transcriptome analysis to obtain transcript patterns specific for NP and ETC. Adequate fixation and embedding methods were established in order to maintain morphology and RNA integrity in fixed and embedded tissue. We dissected NP and ETC at 8 DAF (i.e. within the intermediate phase of caryopsis development), representing the switch from the cellularization/differentiation phase to storage product accumulation (Sreenivasulu et al., 2004). This developmental stage ensures persisting assimilate release and uptake function of NP and ETC, respectively, but also ongoing adjustment of the two nursing tissues to the strong increase of sink strength of the endosperm at the beginning of the filling phase (Weschke et al., 2000). Our transcriptome analysis of NP and ETC revealed tissue-specific hormonal influences on regulatory networks of cellular differentiation and function.

RESULTS

Fidelity of mRNA Amplification

To evaluate the fidelity of T7-RNA polymerase-based mRNA amplification, cDNA array experiments were performed. RNA was extracted conventionally (Sreenivasulu et al., 2002) from frozen grains (8 DAF). Purified RNA (35 μg) was taken for second-strand labeling with [^{33}P]CTP (Sreenivasulu et al., 2006) and used as a reference probe for hybridizations based on the T7 amplification procedure.

T7-based RNA amplification started with 50 ng of total RNA from frozen 8-DAF caryopses. After extraction and a first round of amplification, probes were labeled with [^{33}P]UTP during the second round and hybridized to the barley 12K array. Signal intensities of labeled probes from two independent second-round amplifications were compared with the reference. Rare scatter indicates high concordance of gene expression levels (Fig. 1A), reflected by correlation coefficients of 0.85 and 0.86 for the first and second experiments. Correlation coefficients correspond to overlapping expression of 80% to 82% (Supplemental Table S1). High reproducibility of the two independent amplifications is shown by the scatterplot in Figure 1B and a correlation coefficient of 0.98.

Influence of Fixation and Embedding on RNA Quality and Gene Expression

Fixation and embedding complicates the extraction of high-quality RNA and requires a compromise between histological tissue integrity and RNA quality. Using low-melting-point Steedman's wax avoided high temperatures and significantly improved the preservation of morphology compared with paraffin. We compared different chemical fixatives to examine RNA quality after extraction and amplification. For RNA quality assessment and expression analysis from chemically fixed material, complete caryopses were sectioned and dewaxed. Only ethanol/acetic acid (EAA) fixation resulted in acceptable RNA integrity, whereas formalin-based or ethanol (75%) fixation failed to deliver sufficient RNA quality (data not shown). Total RNA extracted after EAA fixation and dewaxing revealed intact RNA with distinct fluorescent peaks and electrophoretic bands of 18S and 28S ribosomal subunits (Fig. 2). After the first round of amplification, antisense RNA (aRNA) displayed a size distribution from 300 to 2,000 nucleotides, with a maximum between 500 and 1,000 nucleotides (Fig. 2B).

To analyze influences of fixation and embedding, gene expression levels of labeled probes generated from extracted RNA of fixed tissue sections were compared with those of untreated reference probes (shock-frozen grains). Correlation coefficients of 0.77 for two independent biological replicates corresponded to overlapping expression of 72% to 74% of the genes (Fig. 1C; Supplemental Table S1). High correlation of independent biological replicates (r = 0.94) of EAA-fixed sections (Fig. 1D) demonstrated marginal effects of fixation and embedding on the reproducibility of expression data. These experiments indicate that high-quality probes were generated from fixed tissue sections, reproducing more than 70% of the reference transcriptome.

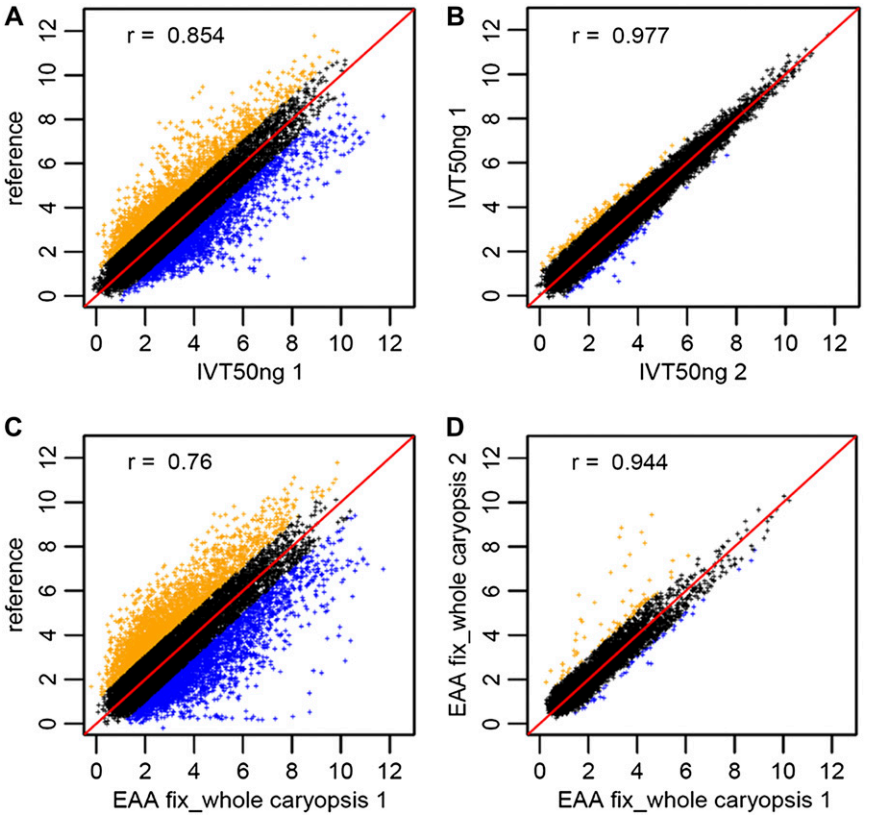

Figure 1. Fidelity of expression signals obtained after hybridization of amplified and nonamplified probes. Representative scatterplots of $\log_2$-transformed signal intensities display correlation between the different probes. The orange- and blue-shaded regions indicate more than 2-fold differences between signal intensities. A, Comparison of a two-round amplification with 50 ng of input RNA to a nonamplified probe with 35 μg of RNA (reference) from a common source. B, Reproducibility of independent two-round amplifications with 50 ng of input from a common source. C, Comparison of a probe from EAA-fixed sections of a completely sectioned caryopsis after two rounds of amplification with 50 ng of input RNA with a nonfixed and nonamplified reference probe from a caryopsis of the same developmental stage with 35 μg of input RNA. D, Reproducibility of expression values from two independent biological replicates of EAA-fixed sections of completely sectioned caryopses.

Expression Analysis of NP and ETC

Figure 3 shows the targeting and marking of NP cells (A), cutting (B) and catapulting (C) of cells with a laser beam, and collection of cuttings (D). LMPC-based expression profiling was performed with dissected tissues to compare maternal NP and filial ETC obtained by the same procedure. RNA, extracted from 25 to 50 cuttings, corresponds to 10,000 to 20,000 cells of NP and 4,000 to 8,000 cells of ETC. Thirty nanograms of total RNA could be extracted from each probe set (Table I). Each probe yielded more than 400 ng of aRNA after the first round of amplification and around 1.6 μg of aRNA after the second round, sufficient amounts to perform high-throughput expression analyses, which commonly require 1 to 2 μg of mRNA or mRNA copies (Duggan et al., 1999; Richmond and Somerville, 2000). The transcriptome data of NP and ETC were surveyed for those candidate genes showing significantly different levels of mRNA expression. Although both tissues are responsible for endosperm supply, nutrient transport is based on different underlying mechanisms, with releasing functions of NP and active, proton-coupled assimilate uptake of ETC. Furthermore, the tissues have a different genetic background: NP is of maternal origin, whereas ETC belongs to the filial tissues. So we were interested in regulatory programs reflecting and determining those differences and focused on data analysis and interpretation of differentially expressed genes. Transcripts were defined as up-regulated by expression ratios $\geq$3 between NP and ETC. In total, 815 genes were identified as differentially expressed (409 genes up-regulated in NP, 406 genes up-regulated in ETC).

Validation of Macroarray Results by Quantitative Real-Time PCR and in Situ Hybridization

Quantitative validation of cDNA array expression data was performed using quantitative real-time (qRT)-PCR. Ratios of signal intensities from selected genes in NP and ETC are compared in Table II. Real-time PCR and macroarray data exhibited remarkable concordance in quantitative ratios between NP and ETC, confirming the reliability of cDNA array analysis with probes extracted by LMPC. Expression of *Nucellin* and *HvPIP1;3* in ETC was only detected on the array, but not by qRT-PCR, possibly due to cross-hybridization of related sequences on the array, pointing to the presence of gene families in barley.

Two tissue-specific genes were selected to confirm the spatial precision of the LMPC procedure by in situ hybridization. The mRNA of *Jekyll*, a potential regulator of NP development (Radchuk et al., 2006), was found to be specifically and highly expressed in NP cells at 8 DAF (Fig. 4, A and B). As in maize (Hueros et al., 1999), the barley ortholog of *BETL4* was shown to be specifically expressed in ETC (Fig. 4, C and D).

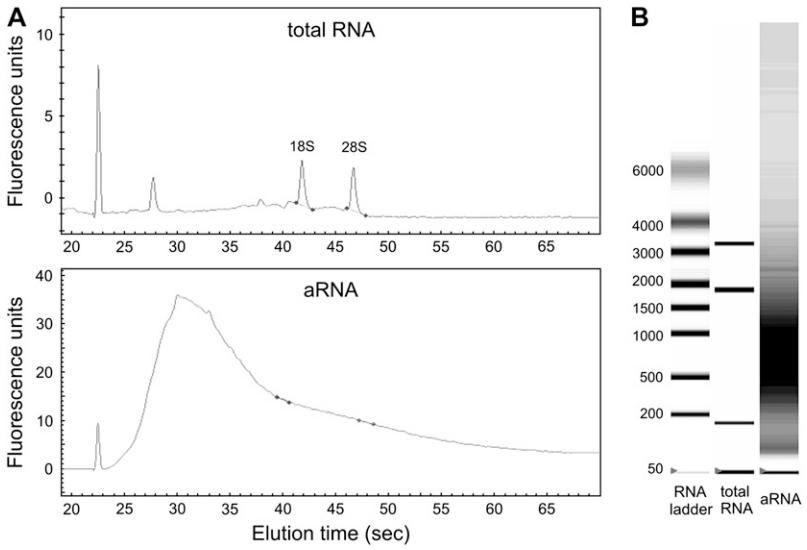

Figure 2. Representative examples of RNA quality from EAA-fixed probes. A, Electropherograms of total RNA and aRNA after one round of amplification. B, Corresponding gel-like images. RNA was extracted from EAA-fixed and Steedman's wax-embedded sections.

Functional Categories of Genes Differentially Expressed in NP and ETC

Genes differently expressed in NP and ETC were annotated and arranged into functional categories (Table III), as described by Sreenivasulu et al. (2006). Twelve functional categories of genes (given in boldface in Table III) are represented by a high number of candidate genes. Genes in seven of the categories are specific for NP. Transcripts related to amino acid metabolism (13 genes) and transport (14 genes) are strongly up-regulated in NP. Furthermore, transcripts associated with DNA synthesis/chromatin remodeling, protein synthesis, secondary metabolism, abiotic stress, as well as secondary metabolism are preferentially expressed in NP. The categories cell wall metabolism, protein degradation, regulation of transcription, and signaling are highly represented in both tissues, indicating activation of related biochemical or regulatory pathways. Only the category hormone metabolism is represented by a higher number of genes in ETC compared with NP. Nearly 40% of differentially expressed genes could not be assigned (113 genes in NP, 205 genes in ETC).

Morphology of NP and ETC at 8 DAF

High numbers of genes preferentially expressed in NP indicate specific functions and/or structural heterogeneity, as revealed by morphological analysis (Fig.

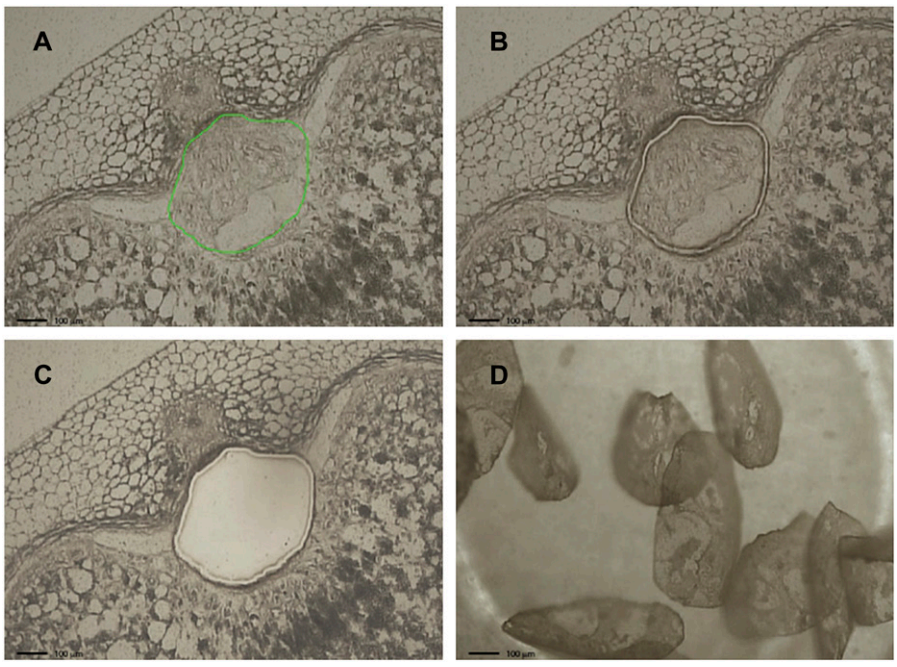

Figure 3. LMPC of the NP (green outline in A) from 20-μm cross sections of EAA-fixed barley caryopses mounted on PEN membrane slides. A, Morphological preservation provides the ability for routine target identification. B, Section after cutting. C, Section after pressure catapulting. D, Dissected NPs captured on the adhesive cap. Bars = 100 μm.

Table I. *Yields of total and amplified RNA from LMPC-captured cells*
Data are averages of three independent experiments.

Cell Source	Total RNA Yield	aRNA after One Round	aRNA after Two Rounds[a]
		ng	
NP	32.7 ± 11.7	434.1 ± 138.0	1,600
ETC	34.3 ± 4.2	456.7 ± 165.2	

[a]Single experiment with probe labeling in the third amplification round.

5). NP is a heterogeneous tissue consisting of three different zones and at least four different cell types (Fig. 5): (1) an upper zone with meristematic cells undergoing active cell division (Fig. 5C, arrows); (2) a middle zone with differentiating/elongating cells (cells in the bottom left corner of Fig. 5C); and (3) the bottom zone with autolysing cells positioned adjacent to the endosperm cavity (Fig. 5D, arrows) and cells showing wall ingrowths (thick-walled cells, arrows in Fig. 5E; electron micrographs of wall modifications are shown in Weschke et al., 2000). In contrast to NP, ETC shows a uniform structure consisting of two or three layers of differentiated cells (Fig. 5B).

Transcriptional Activation of GA Metabolism in NP and Ethylene Metabolism in ETC Correlates with the Expression of Specific Transcription Factors

Hormone metabolism and transcriptional regulation are represented by up-regulation of different classes of genes in both tissues (Table IV). GA and ethylene metabolism are up-regulated in NP and ETC, respectively. Expression of genes involved in hormone biosynthesis as well as catabolism occurs simultaneously, indicating fine-tuning of hormonal functions in both tissues. Table IV shows transcription factors specifically expressed in either NP or ETC. An *AGAMOUS-LIKE* (*AGL*) MADS box gene is preferentially expressed in NP, potentially connected to GA metabolism. In Arabidopsis, GA2ox6 is induced in response to AGL15, and coprecipitation of both proteins in chromatin immunoprecipitation experiments was shown (Wang et al., 2004). Corresponding to transcriptional activation of ethylene metabolism, a group of AP2/EREBP transcription factors is transcriptionally up-regulated in ETC. In Arabidopsis, AP2 functions not only in floral meristem boundary formation and the establishment of floral organ identity but also in developing seeds, probably controlling seed mass and yield (Jofuku et al., 2005; Ohto et al., 2005).

Genes Related to Different Types of Regulated Proteolysis Are Transcriptionally Activated in NP and ETC

Protein degradation seems to be a common regulatory phenomenon in NP and ETC, suggested by high numbers of expressed genes related to ubiquitin ligases (Table V) and proteolysis (Fig. 6). Differences in ubiquitin proteasome subunit gene expression indicate different modes of protein degradation. First, ubiquitin transcripts, up-regulated in ETC, together with ubiquitin-degrading enzymes (ubiquitin C-terminal hydrolase; Table V) suggest a high degree of ubiquitin turnover. Second, transcripts of ubiquitin-activating ligase E1 are preferentially expressed in NP, whereas expression of ubiquitin-conjugating ligase E2 is pronounced in ETC. E3 ubiquitin ligases mediate covalent attachment of ubiquitin to substrate proteins and determine the specificity of degradation. E3 ligases of the Skp1, Cullin, F-box (SCF) complex play a role in hormonal control of the ubiquitin proteasome (Stone and Callis, 2007) and are expressed in both tissues. In NP, a F-box ligase (*SCF*; Table V) and a *GRAS* family transcription factor (Table IV) are more than 10-fold up-regulated. GRAS proteins with DELLA domains are substrates of F-box E3 ligases acting in the GA transduction pathway (Sun and Gubler, 2004). Also characteristic for NP is transcriptional activation of C3HC4-type ring finger ligases (Table V). In ETC,

Table II. *Validation of macroarray expression data by qRT-PCR*
The values listed in the two columns at right are the ratios of signal intensities between NP and ETC as quantified by macroarray analysis and real-time PCR.

Clone ID[a]	Gene	Ratio NP Versus ETC	
		Macroarray	Real-Time PCR
HY09L21	Jekyll[b]	64.0	51.1
HA23G24	HvPIP1;3	7.2	nd[c]
HY09L18	Nucellin	3.9	nd[c]
HB02D13	BETL4	−11.3	−5.9
HB05H15	Invertase inhibitor	−41.1	−95.9
HB31C12	α-Amylase/subtilisin inhibitor	−43.7	−87.4
HZ42M04	Hypothetical protein[d]	−2.2	1.1

[a]Identifier number from the IPK Crop EST Database (http://pgrc.ipk-gatersleben.de/cr-est). [b]Regulator gene of NP development (Radchuk et al., 2006). [c]nd, Not detected in transfer cells by qRT-PCR. [d]Hypothetical protein similar to Ac1147 from *Rattus norvegicus*.

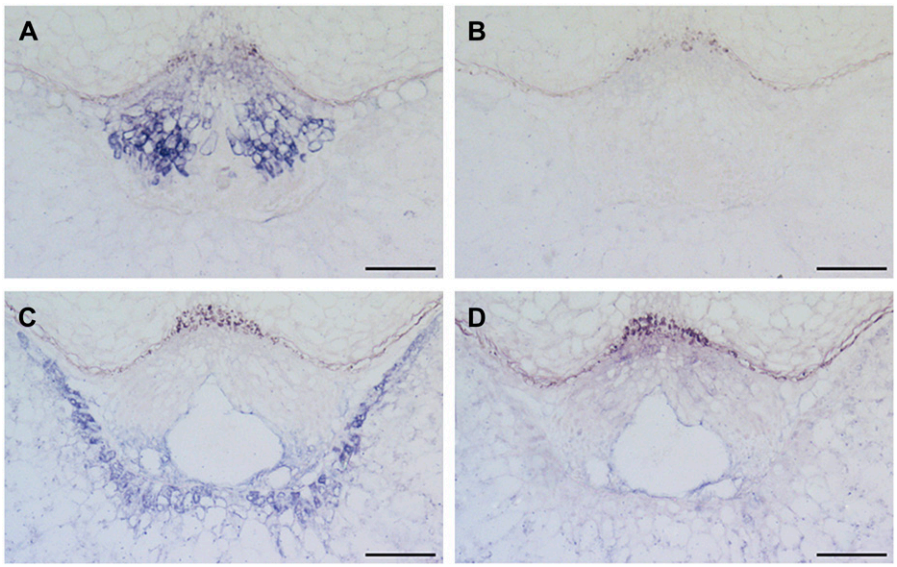

Figure 4. Localization of mRNA of tissue-specific transcripts by in situ hybridization. Antisense probes of *Jekyll* (A) and *BETL4* (C) indicate preferential expression in NP and ETC, respectively. B and D show the regions from A and C, respectively, after hybridization with sense probe for a negative control. Bars = 100 μm.

ethylene metabolism is up-regulated (Table IV). EIN3-binding F-box 1- and 2-forming ubiquitin protein ligases in Arabidopsis repress ethylene action and promote growth by directing EIN3 degradation (Gagne et al., 2004). In agreement with that, *EIN3* was not up-regulated in ETC. A *DD1* gene, up-regulated in ETC (Fig. 6), belongs to the S locus F-box genes (*SLF*/*SFB*) associated with protein ubiquitination via E3 ubiquitin ligases (Vierstra, 2003). A group of *DD* genes (*DD1–DD10*) is expressed in *Nicotiana alata* pollen (Wheeler and Newbigin, 2007).

Proteases Preferentially Expressed in NP Are Associated with PCD

Protease genes related to PCD, such as subtilisin-like Ser proteinases and Cys and Asp endopeptidases (Beers et al., 2000), are predominantly up-regulated in NP, although some transcripts of related types were also up-regulated in ETC (Fig. 6). Barley nucellain, an apoplastic peptidase of the legumain-type peptidase family C13 (Chen et al., 1997), is transcriptionally up-regulated in NP. The protein is localized in degenerating cell walls of the nucellus (Linnestad et al., 1998) and is not related to Cys peptidases of the papain family, C1 (Rawlings and Barrett, 1994), which are also transcriptionally activated in NP. Peptidases of the papain family correlate to senescence processes in different plant species (Griffith et al., 1997; Guerrero et al., 1998; Noh and Amasino, 1999; Xu and Chye, 1999). Papain-like Cys proteases also play a crucial role in plant-pathogen/pest interaction (Shindo and Van der Hoorn, 2008). *Nucellin*, which is expressed in nucellar cells after pollination, plays a potential role in nucellar degeneration (Chen and Foolad, 1997) and is simultaneously up-regulated in NP with a second aspartic protease of the phytepsin type. Phytepsins exhibit a high similarity to animal cathepsin D proteins (Runeberg-Roos et al., 1991), linked with PCD (Deiss et al., 1996). Subtilisins, preferentially expressed in NP, play an obvious role in PCD of nucellar and endosperm cells of barley (Young and Gallie, 2000). A caspase-like activity has been described for a subtilisin-like Ser protease, probably involved in the proteolysis of fungus-initiated PCD in *Avena sativa* (Coffeen and Wolpert, 2004). Involvement of caspase-like proteases in PCD was also shown in cells of nucellus of *Sechium edule* seeds (Lombardi et al., 2007).

In NP, amino acid metabolism is stimulated at the transcriptional level, probably connected to proteolysis (Table III). Mitochondrial Gly decarboxylase, Met-γ-lyase, and Gln and Pro dehydrogenases are transcriptionally activated (Table VI), with potential functions in amino acid catabolism. Ala/glyoxylate dehydrogenase and four genes encoding cytosolic isoforms of Gln synthetase are up-regulated, possibly catalyzing the reconversion of amino acids into isoforms suitable for transport. Increased mRNA levels of phospho*enol*-pyruvate carboxylase, aconitate hydratase, and NADP-malic enzyme indicate refixation of released ammonia, a process requiring carbon acceptors in the form of organic acids.

Proteases Expressed in ETC Are Related to Degradation Pathways Associated with Etioplast/Chloroplast Differentiation

The proteolysis-related transcriptome of ETC is highly specific and possibly related to etioplast/chloroplast differentiation pathways. Two transcripts, annotated as ATP-dependent metalloprotease FtsH and ATP-dependent Clp protease, proteolytic subunit (Fig. 6), play crucial roles in etioplast and chloroplast biogenesis (Kanervo et al., 2008). FtsH-type ATP-dependent metalloproteases are potentially involved in fine-tuning of cytochrome b_6f complex synthesis and can

Table III. *Functional categories of up-regulated genes in NP (409 genes) and ETC (406 genes)*

Transcripts with estimated changes of 3-fold or greater were functionally annotated according to Sreenivasulu et al. (2006). Overrepresented categories are given in boldface. Categories were defined as overrepresented according to the number of genes representing more than 2% of the total number of up-regulated genes in each tissue. CHO, Carbohydrate.

Functional Category	No. of Up-Regulated Genes in NP	No. of Up-Regulated Genes in ETC
Amino acid metabolism	**13**	4
Cell wall metabolism	**16**	**17**
Glycolysis	3	1
Fermentation	0	2
Lipid metabolism	7	2
Minor CHO metabolism	1	6
Major CHO metabolism	3	1
Nitrogen metabolism	6	0
Nucleotide metabolism	6	0
Oxidative pentose phosphate	1	0
Photosynthesis	0	2
Secondary metabolism	**9**	4
TCA	3	1
Cell organization	3	8
Development	4	5
DNA synthesis/chromatin structure	**45**	6
Protein synthesis	**34**	7
Protein targeting	4	3
Posttranslational modification	**11**	8
Protein degradation	**32**	**31**
Redox	0	4
RNA regulation of transcription	**21**	**26**
RNA processing	3	2
Signaling	**10**	**9**
Hormone metabolism	7	**10**
Stress, abiotic	**17**	6
Stress, biotic	4	4
Transport	**14**	7
Miscellaneous	**19**	**25**
Not assigned	**113**	**205**

degrade unassembled proteins (Ostersetzer and Adam, 1997). Like FtsH proteases, Clp protease complexes are transcriptionally activated during the etioplast-to-chloroplast transition; however, their role seems unclear. Similar to the FtsH and Clp protease complexes, DEG proteases are involved in the degradation of damaged and misfolded proteins. In Arabidopsis, DEG proteins are activated after light-induced damage of the D1 protein from the reaction center of PSII (Sun et al., 2007). A gene encoding a DEGP protease-like transcript shows stimulated expression in ETC (Fig. 6).

A nucleotide sequence encoding Cys protease Mir1 is also expressed in ETC (Fig. 6). Mir1-CP is a defense-related Cys protease accumulating in insect-resistant maize genotype Mp708, obviously connected to ethylene synthesis and perception (Harfouche et al., 2006).

Different Types of Cell Wall Synthesis Are Stimulated in NP and ETC

Transcript analysis of NP and ETC indicates the stimulation of cell wall synthesis. In ETC, up-regulated *UDP-glucose pyrophosphorylase*, *phosphomannomutase*, and two isoforms encoding GPD-Man pyrophosphorylase (Table VI) may provide GDP-Man, the activated form of Man, for incorporation into cell wall products. Stimulated expression of *β-mannan synthase* and *α-mannosidase* supports this view. Strong up-regulation of genes encoding pectinesterases, α-galactosidases, and different glucosidases gives further hints to activated cell wall metabolism and/or turnover (Table VI). Increased mRNA levels for expansin and extensin suggest stimulated cell expansion. Interestingly, two genes encoding type II trehalose-6-P synthase/phosphatase (TPS/TPP) show strong up-regulation (up to 15-fold) in transfer cells compared with the NP.

Genes encoding *S*-adenosyl-L-homo-Cys hydrolase and *S*-adenosyl-Met synthetases 1 and 4 are preferentially expressed in NP (Table VI). *S*-Adenosyl-Met may be required for cell wall biosynthesis, because impaired recycling affected the degree of methylesterification in Arabidopsis cell walls (Pereira et al., 2006). Up-regulated genes encoding Suc synthases 1 and 2 can supply the primary sugar nucleotides for cell wall synthesis, UDP-D-Glc, the substrate for cellulose synthase, which also shows transcriptional activation. Two up-regulated isoforms of *UDP-D-glucuronate decarboxylase* may catalyze the synthesis of UDP-Xyl from UDP-glucuronate synthesis, and up-regulated forms of *arabinoxylan arabinofuranohydrolase* and *α-L-arabinofuranosidase* could be involved in the metabolism of arabinoxylans derived from UDP-Xyl. The most strongly up-regulated genes encode β-expansins, with a suggested role in cell expansion.

NP and ETC Show Differences in Transporter Gene Activity

Compared with ETC, the spectrum of preferentially expressed transporter genes in NP cells is less defined with regard to substrate specificity (Table VII). Several aquaporin members were up-regulated in NP. Plant aquaporins are classified into plasma membrane intrinsic proteins (PIPs), tonoplast intrinsic proteins (TIPs), NOD26-like intrinsic proteins, and small basic intrinsic proteins. Four PIP (*HvPIP1;1*, *HvPIP1;3*, *HvPIP2;2*, and *HvPIP2;5*) and two TIP genes, belonging to subclasses 1 and 2 (representing δ- and γ-TIPs), were highly expressed in NP (Table VII). Other up-regulated transporter genes in NP show high similarity to voltage-dependent anion channels (VDAC2) of wheat (*Triticum aestivum*) and to a metal transporter of rice (*Oryza sativa*).

In contrast to NP, genes encoding transporters with more defined substrate specificities are up-regulated in ETC. All catalyze the proton-coupled active transfer of solutes. *SUCROSE TRANSPORTER1* (*HvSUT1*) is

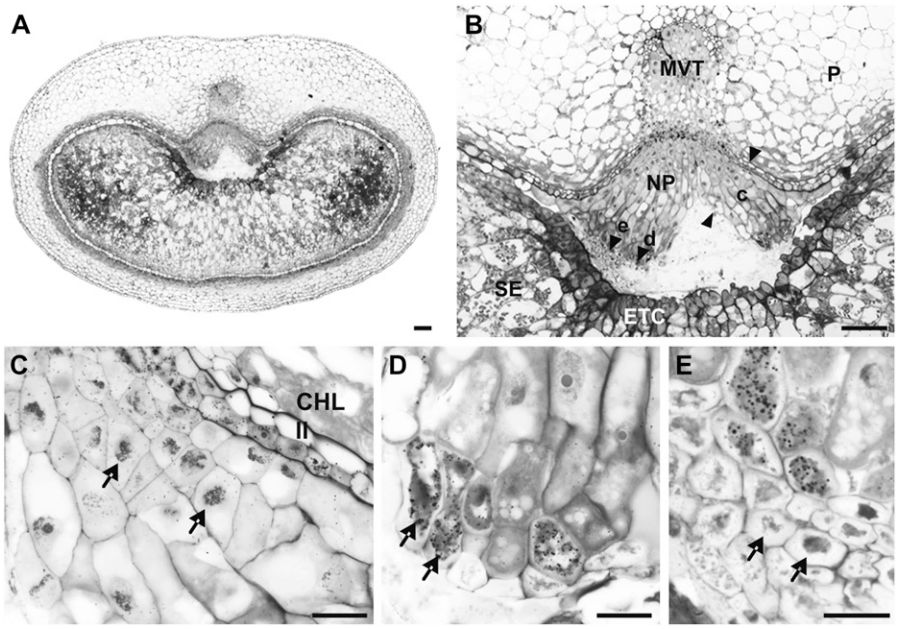

Figure 5. Different regions of the NP of a barley grain at 8 DAF as defined by morphological features. A and B, Median cross section of a barley caryopsis (A) and magnification of the maternal-filial boundary consisting of NP and ETC (B). Arrowheads labeled c, d, and e mark different cell types shown in higher magnification (in C–E). C, Upper region of the NP with actively dividing cells (arrows). D, Apoptotic bodies (arrows) in cells undergoing autolysis adjacent to the endospermal cavity. E, Bottom part of the NP with transfer cell-like structures showing cell walls of enormous thickness (arrows). CHL, Chlorenchyma; II, inner integument; MVT, main vascular tissue; P, pericarp; SE, starchy endosperm. Bars = 100 μm (A and B) and 20 μm (C–E).

expressed in ETC and at lower levels in thick-walled cells of NP (Weschke et al., 2000). Barley HAK2 is a low-affinity, Na^+-sensitive K^+ transporter, acting in tonoplasts to mediate K^+ transfer from vacuoles to cytoplasm, thereby avoiding K^+ starvation (Senn et al., 2001). Other up-regulated genes in ETC (Table VII) encode putative amino acid permeases (AAPs; HA16M17 and HZ36G22) and a putative nitrate transporter (HZ48O07).

Database analysis (HarvEST: Barley v1.63; www.harvest-web.org; Close et al., 2007), using amino acid sequences of functionally characterized transport proteins of Arabidopsis and *Vicia faba* as reference sequences, revealed that AAPs consist of at least 10 members in barley (Fig. 7). AAPs functionally characterized in barley (C. Seiler, unpublished data) are assigned as HvAAP1 and HvAAP2. The phylogenetic tree shows that AAPs up-regulated in ETC (HA16M17

Table IV. *Differentially expressed genes involved in hormone metabolism and transcriptional regulation*

Genes with expression ratios ≥3 between NP and ETC as quantified by macroarray analysis. Positive values indicate up-regulation in NP, and negative values indicate up-regulation in ETC.

Clone ID[a]	Fold Change	Gene Identification [Species]	BLASTX Score[b]
Hormone metabolism			
HZ65M10	58.4	*ent*-Kaurene synthase-like 2 [*Oryza sativa*]	105
HZ48M23	7.4	GA 2-oxidase 5 [*Hordeum vulgare*]	295
HZ59P09	6.5	Lipoxygenase 1 (LOX1) [*Hordeum vulgare*]	332
HA01N04	4.7	Auxin-regulated protein [*Arabidopsis thaliana*]	112
HB08G15	−8.2	Ethylene-forming enzyme-like protein [*Arabidopsis thaliana*]	199
HB30I05	−4.6	ACC oxidase-like protein [*Arabidopsis thaliana*]	138
HY04L15	−3.3	Putative ACC deaminase [*Oryza sativa*]	296
Transcriptional regulation			
HY04L24	12.0	Putative GRAS family transcription factor [*Oryza sativa*]	214
HY06M13	8.5	AGAMOUS-like protein 2 (HvAG2) [*Hordeum vulgare*]	252
HA16M02	12.7	MADS box protein ZMM17 [*Zea mays*]	249
HZ48O08	3.9	MADS box protein 9 [*Hordeum vulgare*]	363
HB03O23	3.2	MADS box protein [*Triticum aestivum*]	346
HY03I16	−7.7	Putative AP2/EREBP transcription factor [*Arabidopsis thaliana*]	91
HZ57B05	−13.2	AP2 domain-containing protein [*Oryza sativa*]	33
HA03G10	−3.3	Putative transcription factor EREBP1 [*Oryza sativa*]	201
HA06K23	−3.4	AN1-like zinc finger [*Oryza sativa*]	283

[a]Identifier number from the IPK Crop EST Database (http://pgrc.ipk-gatersleben.de/cr-est). [b]BLASTX searches were performed in April 2008.

Table V. *Differentially expressed genes of the ubiquitin proteasome system*
For details, see Table IV.

Clone ID[a]	Fold Change	Gene Identification [Species]	BLASTX Score[b]
HA22J22	8.0	Ubiquitin-activating enzyme E1 [*Triticum aestivum*]	334
HY05H21	4.1	Ubiquitin-activating enzyme E1 [*Oryza sativa*]	207
HA31B05	3.5	Ubiquitin-activating enzyme E1 [*Triticum aestivum*]	377
HZ60D04	18.2	F-box family E3 (SCF) [*Arabidopsis thaliana*]	56
HZ49E24	29.5	Zinc finger, C3HC4 type (RING) [*Arabidopsis thaliana*]	67
HY05P10	15.4	Putative zinc finger, C3HC4-type E3 (RING) [*Oryza sativa*]	217
HA15F12	5.3	Putative zinc finger, C3HC4-type E3 (RING) [*Arabidopsis thaliana*]	97
HY06O13	5.1	Putative zinc finger, C3HC4-type E3 (RING) [*Oryza sativa*]	107
HY08P12	3.0	Similar to Pspzf zinc finger protein E3 (RING) [*Arabidopsis thaliana*]	59
HY10J14	2.9	Protein F2D10.27 E3 (RING) [*Arabidopsis thaliana*]	79
HA12M15	−3.3	Ubiquitin-conjugating enzyme E2 [*Oryza sativa*]	308
HA16E24	−3.0	Putative ubiquitin-conjugating enzyme E2 [*Oryza sativa*]	145
HB14C03	−2.9	Putative ubiquitin-conjugating enzyme E2 [*Arabidopsis thaliana*]	305
HA07J02	−2.8	Putative ubiquitin-conjugating enzyme E2 [*Arabidopsis thaliana*]	308
HB07K14	−4.7	Copine I-like E3 (RING) [*Oryza sativa*]	149
HA01B21	−7.2	Leu-rich repeat protein E3 (SCF) [*Oryza sativa*]	225
HA02I11	−3.3	Putative Skp1 family protein E3 (SKP) [*Oryza sativa*]	358
HB23B05	−4.0	Polyubiquitin 6 [*Oryza sativa*]	345
HF08N09	−4.1	Polyubiquitin (UBQ3) [*Nicotiana tabacum*]	44
HA30L14	−5.4	Polyubiquitin [*Pinus sylvestris*]	285
HF12F18	−9.1	Polyubiquitin [*Elaeagnus umbellata*]	343
HY09O04	−3.3	Putative polyubiquitin (UBQ10) [*Arabidopsis thaliana*]	351
HY10I04	−2.8	Polyubiquitin 2.3_cis2 his2-zinc finger [*Mus musculus*]	116
HB17D20	−4.6	Putative ubiquitin C-terminal hydrolase [*Oryza sativa*]	94
HF03K09	−3.3	Ubiquitin C-terminal hydrolase [*Oryza sativa*]	303

[a]Identifier number from the IPK Crop EST Database (http://pgrc.ipk-gatersleben.de/cr-est). [b]BLASTX searches were performed in April 2008.

belongs to 35_776 consensi and HZ36G22 belongs to 35_779 consensi, given in boldface) cluster into different branches. 35_776 shows a close homology to the cluster of functionally characterized AtAAP1 (Hirner et al., 1998), AtAAP6, and AtAAP8 (Okumoto et al., 2002). 35_779 is more distantly related to this cluster but shows close similarity to HvAAP1. Using the same HarvEST assembly (data not shown), HZ48O07 was shown to be related to Arabidopsis nitrate transporter 1.1, a dual-affinity transporter for nitrate and chlorate, which influences the timing of seed dormancy and germination (Alboresi et al., 2005).

DISCUSSION

LMPC-based transcriptome analysis focused on the two transfer tissues NP and ETC. The main results are schematically summarized in Figure 8 and will be discussed below.

LMPC-Based Transcriptome Analysis Was Adapted to Developing Barley Grains

To use LMPC-coupled transcriptome analysis in developing barley grains, we first established methods for fixation and embedding to maintain morphology and RNA integrity in fixed, embedded tissue. EAA fixation combined with embedding in Steedman's wax preserved morphological integrity and provided RNA of sufficient quality as well. We could show that two rounds of T7-based RNA amplifications largely maintain the relative abundance of the original mRNA population, similar to results in mammalian systems (Nygaard and Hovig, 2006). Probes from fixed tissue sections for cDNA array analysis reflected the reference transcriptome to more than 70%. The comparison of gene expression profiles performed for NP and ETC revealed specific regulatory networks of cellular differentiation and function as well as potential control patterns by hormonal pathways.

The Function of NP Involves Hormonal Regulation by GA

The NP consists of mitotically active, differentiating/elongating as well as disintegrating cells, forming a top-down differentiation gradient, which is present throughout grain development. The high transcriptional activity of GA metabolism suggests a role in establishing and maintaining this differentiation gradient. Mitotic activity in NP is indicated by the high amount of mRNA of different histones (Supplemental Table S2) and the preferred expression of C3HC4-type ring finger ubiquitin ligases (Table V), which are known to play a key role in cell cycle regulation of

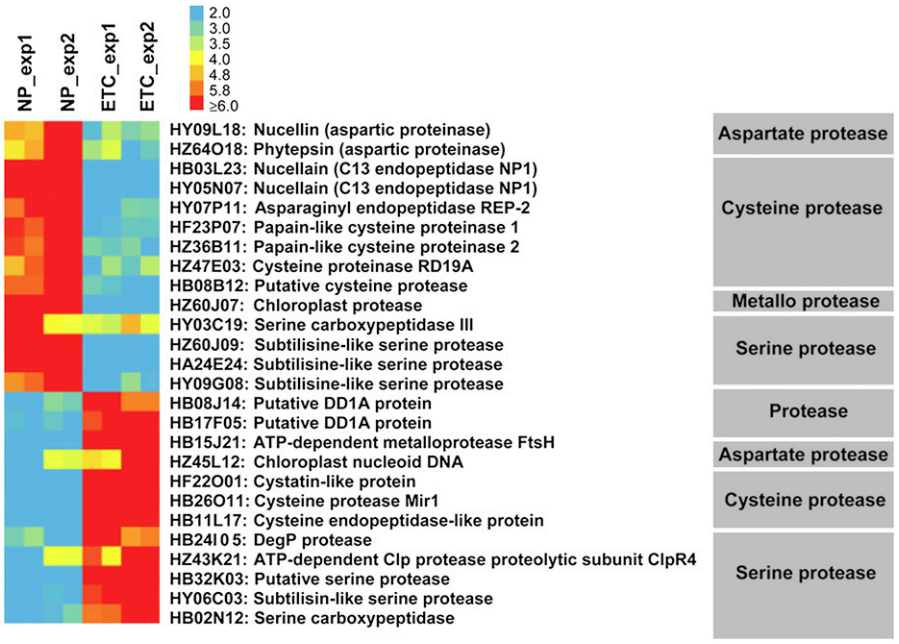

Figure 6. Expression pattern of members of protease gene families in NP and ETC. Expression levels of NP and ETC from two independent biological replicates (exp1 and exp2) are indicated in color scale (normalized expression values): red, high expression; yellow, moderate expression; blue, low expression (see also color scale at the top). EST identity numbers, putative BLAST descriptions, and functional categories are given at right.

Arabidopsis (Fleury et al., 2007; Liu et al., 2007). On the other hand, biologically active GAs in NP seem to be involved in the elongation of cells, as proposed for embryo axis formation in *Brassica napus* (Hays et al., 2002), underlining the role of GA in phase transitions, such as the shift from juvenile to adult development and the transition from vegetative to generative development (Scott et al., 1999; Sakamoto et al., 2001). GA levels are regulated by catabolic GA 2-oxidases, which are in Arabidopsis transcriptionally activated together with AGL15 (Wang et al., 2004). On the other hand, homeotic genes like *AGAMOUS* are reported to be positive regulators of the GA pathway. Parallel activation of *GA4* encoding an enzyme catalyzing the production of bioactive GAs (Williams et al., 1998) and *AGAMOUS* during carpel and stamen development of Arabidopsis suggests that AGAMOUS induces GA biosynthesis, at least during organogenesis (Gomez-Mena et al., 2004). The authors propose a general role for GA in the transition from meristem identity to organogenesis. We conclude that fine-tuning of GA activity by GA biosynthesis and catabolism together with AGL activity may regulate the transition from mitosis to cell elongation from the upper to the middle part of NP.

Within NP, strong up-regulation of genes involved in amino acid catabolism and ammonia refixation (Table III) indicates protein degradation and remobilization of nitrogen, which corresponds to massive cell degradation in the bottom part of NP (Fig. 5D, arrows). Degradation processes in the NP are developmentally regulated (Radchuk et al., 2006) and probably induced by endosperm growth. Specific types of proteases expressed in the NP (Fig. 6) are potentially involved in PCD-like processes. Conversion of cells into "apoptotic bodies" (Adrain and Martin, 2001; Fig. 5D) and expression of caspase-like activities (Fig. 6) relate PCD of NP cells to apoptosis (Reape et al., 2008).

In summary, relation of the differentiation gradient to transcriptional activation in NP strongly suggests that GA plays a major role in developmental regulation and that cell disintegration is initiated by PCD-related remobilization processes.

Transporters Expressed in NP and ETC Are Involved in Nitrogen Remobilization and Amino Acid Transfer

Six up-regulated genes in NP belong to the aquaporin family. In French bean (*Phaseolus vulgaris*), three PIP genes are expressed in the seed coat ground parenchyma proximal to the vascular bundles, with a potential role for nutrient efflux from seed coats (Zhang et al., 2007). Thus, up-regulated PIP genes could be involved in solute efflux from NP cells into the apoplast. Two members of TIPs are strongly up-regulated in NP (δ-type TIP2;3 more than 21-fold; Table VII). TIP isoforms are possibly localized to different vacuolar compartments, but the distinct assignment to specific subcellular compartments remains unclear. Earlier studies in root cells postulated that α- and/or δ-TIPs are predominantly located in protein storage vacuoles, whereas lytic vacuoles are enriched in γ-TIPs (Jauh et al., 1998, 1999). More recently, all three TIP isoforms were shown to be localized to the tonoplast of the central vacuole in Arabidopsis leaves and mature roots (Hunter et al., 2007). Notably in senescing leaves, a high enrichment of γ-TIPs in the tonoplast of the central vacuole was visualized (Otegui et al., 2005). During Arabidopsis seed development, α-TIPs were exclusively found in developing embryos restricted to protein storage vacuoles, whereas δ- and γ-TIP expression was observed

Table VI. *Differentially expressed genes involved in nitrogen metabolism and cell wall metabolism*
For details, see Table IV.

Clone ID[a]	Fold Change	Gene Identification [Species]	BLASTX Score[b]
Nitrogen metabolism			
HY04F14	11.2	Gly decarboxylase P (mitochondrial) [*Arabidopsis thaliana*]	358
HZ64B13	4.7	Pro dehydrogenase [*Oryza sativa*]	69
HY06D11	3.1	Met-γ-lyase [*Oryza sativa*]	203
HF06E08	7.1	Ala:glyoxylate aminotransferase [*Arabidopsis thaliana*]	108
HY07D14	17.2	Glu dehydrogenase [*Oryza sativa*]	213
HA27K11	6.5	Gln synthetase 1 [*Oryza sativa*]	320
HZ59K18	5.1	Gln synthetase GSe2 [*Triticum aestivum*]	244
HZ57P11	3.3	Gln synthetase (cytosolic) [*Hordeum vulgare*]	325
HA07K13	3.3	Gln synthetase GSr1 [*Triticum aestivum*]	305
HY02N02	34.5	Dehydroquinate dehydratase/shikimate 5-dehydrogenase [*Oryza sativa*]	250
HY04G05	28.8	*S*-Adenosyl-L-homo-Cys hydrolase [*Hordeum vulgare*]	217
HF23O03	6.9	*S*-Adenosyl-L-homo-Cys hydrolase [*Hordeum vulgare*]	345
HF15G14	3.1	*S*-Adenosyl-Met synthetase 1 [*Hordeum vulgare*]	355
HY10L08	7.5	*S*-Adenosyl-Met synthetase 4 [*Hordeum vulgare*]	235
HB21G15	3.7	Aconitate hydratase [*Solanum lycopersicum*]	289
HY06L21	4.2	Aconitate hydratase [*Arabidopsis thaliana*]	353
HY06D05	3.1	Phospho*enol*pyruvate carboxylase [*Triticum aestivum*]	376
HF23M12	4.1	NADP-malic enzyme [*Oryza sativa*]	347
Cell wall			
HY01J06	4.7	ADP-Glc pyrophosphorylase [*Hordeum vulgare*]	274
HF11H21	7.5	Suc synthase 1 [*Hordeum vulgare*]	361
HY10D14	4.6	Suc synthase 2 [*Hordeum vulgare*]	419
HB22D22	3.4	Transaldolase [*Oryza sativa*]	315
HY04D24	6.7	UDP-D-glucuronate decarboxylase [*Hordeum vulgare*]	142
HF19D20	3.6	UDP-D-glucuronate decarboxylase [*Hordeum vulgare*]	298
HY10D13	3.1	β-1,3-Glucanase [*Arabidopsis thaliana*]	125
HA08J01	3.1	β-Expansin B2 [*Triticum aestivum*]	239
HZ42H09	30.1	β-Expansin B3 [*Triticum aestivum*]	286
HF11E17	33.8	β-Expansin 7 [*Triticum aestivum*]	158
HB04A14	11.8	Arabinoxylan arabinofuranohydrolase (AXAH-I) [*Hordeum vulgare*]	358
HF04G18	3.8	α-L-Arabinofuranosidase (ARA-I) [*Hordeum vulgare*]	92
HZ47F10	3.4	Cellulose synthase 4 [*Oryza sativa*]	209
HA27J19	3.2	Myoinositol-1-P synthase [*Hordeum vulgare*]	344
HB19F14	−15.1	Trehalose-6-P synthase/phosphatase type II [*Oryza sativa*]	157
HB11P06	−14.5	Trehalose-6-P synthase/phosphatase type II [*Oryza sativa*]	252
HF04F06	−6.2	Putative GDP-Man pyrophosphorylase [*Oryza sativa*]	326
HA08H22	−5.0	Putative GDP-Man pyrophosphorylase [*Oryza sativa*]	274
HA20G11	−3.7	Phosphomannomutase (PMM) [*Oryza sativa*]	266
HB28J16	−3.4	α-Mannosidase [*Oryza sativa*]	227
HB08E12	−6.7	Pectinesterase [*Arabidopsis thaliana*]	94
HA15P24	−12.7	Pectinesterase [*Oryza sativa*]	123
HB23M06	−8.0	β-Mannan synthase [*Oryza sativa*]	84
HZ47K23	−15.1	α-Galactosidase [*Oryza sativa*]	244
HY02A06	−9.1	α-Galactosidase [*Hordeum vulgare*]	216
HA22P03	−13.0	Glucan endo-1,3-β-D-glucosidase [*Hordeum vulgare*]	296
HY02A06	−9.1	α-Glucosidase [*Hordeum vulgare*]	216
HA22E18	−3.1	β-Expansin B15 [*Oryza sativa*]	310
HA13L06	−10.9	Cys-rich extensin [*Nicotiana tabacum*]	31
HB26H01	−7.3	Polygalacturonase [*Oryza sativa*]	118
HY09I24	−3.1	UDP-Glc pyrophosphorylase [*Hordeum vulgare*]	134

[a]Identifier number from the IPK Crop EST Database (http://pgrc.ipk-gatersleben.de/cr-est). [b]BLASTX searches were performed in April 2008.

after germination, probably in the same compartment (Hunter et al., 2007). The TIP isoforms showed a specific temporal expression pattern during embryo maturation and germination, with the presence of α-TIPs very early, transition from α- to γ-TIP expression at 2.5 d after germination, and transition from γ- to δ-TIP 1 d later at 3.5 d after germination. This temporal expression pattern during germination points to the involvement of TIPs in lytic and/or remobilization processes and corresponds to high

Table VII. *Differentially expressed transporter genes*

For details, see Table IV.

Clone ID[a]	Fold Change	Gene Identification [Species]	BLASTX Score[b]
Aquaporins			
HA02B08	12.6	Plasma membrane intrinsic protein (PIP1;1) [*Hordeum vulgare*]	184
HA23G24	7.2	Plasma membrane intrinsic protein (PIP1;3) [*Hordeum vulgare*][c]	285
HA03G06	4.8	Plasma membrane intrinsic protein (PIP2;5) [*Hordeum vulgare*]	199
HA16G04	2.8	Plasma membrane intrinsic protein (PIP2;2) [*Hordeum vulgare*]	340
HY08I05	21.0	Delta-type tonoplast intrinsic protein (TIP2;3) [*Triticum aestivum*]	107
HZ53E01	3.4	Tonoplast intrinsic protein (TIP1/AQP6) [*Triticum aestivum*]	302
Anions			
HF09E15	3.1	Voltage-dependent anion channel 2 (VDAC2) [*Triticum aestivum*]	267
Metal			
HY03F19	5.3	Putative metal-binding protein [*Oryza sativa*]	124
Suc			
HZ64P03	−8.5	Suc transporter 1 (SUT1) [*Hordeum vulgare*]	258
Nitrogen			
HA16M17	−3.3	Amino acid permease 6 [*Arabidopsis thaliana*]	206
HZ36G22	−6.6	Transmembrane amino acid transporter protein [*Oryza sativa*]	242
HZ48O07	−4.7	Nitrate transporter [*Oryza sativa*]	137
Potassium			
HY03H23	−3.8	Potassium transporter 2 (HAK2) [*Hordeum vulgare*]	296

[a]Identifier number from the IPK Crop EST Database (http://pgrc.ipk-gatersleben.de/cr-est). [b]BLASTX searches were performed in April 2008. [c]qRT-PCR was performed.

mRNA levels of δ-TIP2;3 and γ-TIP1/AQP6 in NP of barley seeds. Up-regulated expression of a gene encoding VDAC2 (Table VII), which belongs to the mitochondrial porins and facilitates the transport of anions across mitochondrial outer membranes in wheat (Elkeles et al., 1995), gives further hints for senescence/PCD-associated processes in NP. In mammalian systems, it has been shown that VDACs play an essential role in apoptosis by increasing mitochondrial membrane permeability, which allows the release of apoptogenic factors into the cytoplasm. Anti-apoptotic Bcl-2 protein directly interacts with VDACs and blocks cell death by closing VDACs (for review, see Tsujimoto and Shimizu, 2002). Heterologous expression of a rice VDAC (*OsVDAC4*) in a Jurkat T-cell line induced apoptosis, which could be blocked by Bcl-2 complementation (Goldbole et al., 2003). The authors conclude that plant and animal VDACs share similar functions in PCD pathways and thus are probably conserved mitochondrial elements of death pathways in plant and animal cells.

Transport-associated genes expressed in ETC encode transporters catalyzing proton-coupled cotransport, such as HvSUT1 (Weschke et al., 2000). Two putative amino acid permeases up-regulated in ETC are similar to functionally characterized AAPs from Arabidopsis (35_776_HvAAP; AtAAP1 [Hirner et al., 1998], AtAAP6, and AtAAP8 [Okumoto et al., 2002]) and barley (35_779_HvAAP; C. Seiler, unpublished data; Fig. 7). Expression of these genes confirms the specificity of the developmental stage selected for analysis (8 DAF). Situated within the so-called intermediate or transition phase of seed development (for review, see Weber et al., 2005), processes occurring in NP and ETC reflect the switch from the cell division/elongation phase to storage product accumulation. Characteristic for this developmental stage is the strong increase of *HvSUT1* activity (Weschke et al., 2000) as well as the switch from high to low hexose to Suc ratios in the developing endosperm (Weschke et al., 2000, 2003). Furthermore, genes encoding storage proteins are strongly up-regulated at the transcriptional level (Sreenivasulu et al., 2004). High mRNA levels of putative amino permeases in ETC at the beginning of protein accumulation suggest a role for the uptake of amino acids into the endosperm.

The Ethylene Response in ETC Is Related to Defense Mechanisms and Might Influence Barley Grain Development

Some transcripts up-regulated in ETC are known to be involved in the differentiation of etioplasts/chloroplasts and in light-induced damage of proteins (Sun et al., 2007; Kanervo et al., 2008), despite the fact that ETC are localized within the grain and do not contain green plastids. In barley, transfer cells differentiate from the first epidermal cell row by anticlinal divisions (Olsen, 2001). Epidermal cells typically represent a boundary to adjacent tissues, are responsible for defense reactions, and control differentiation (Becraft, 1999). As observed in ETC, epidermal cells of barley leaves contain transcripts of ATP-dependent FtsH, Clp, and DEG proteases encoded in the leaf epidermis by other members of the gene families. The expression of these genes is induced by infection with powdery

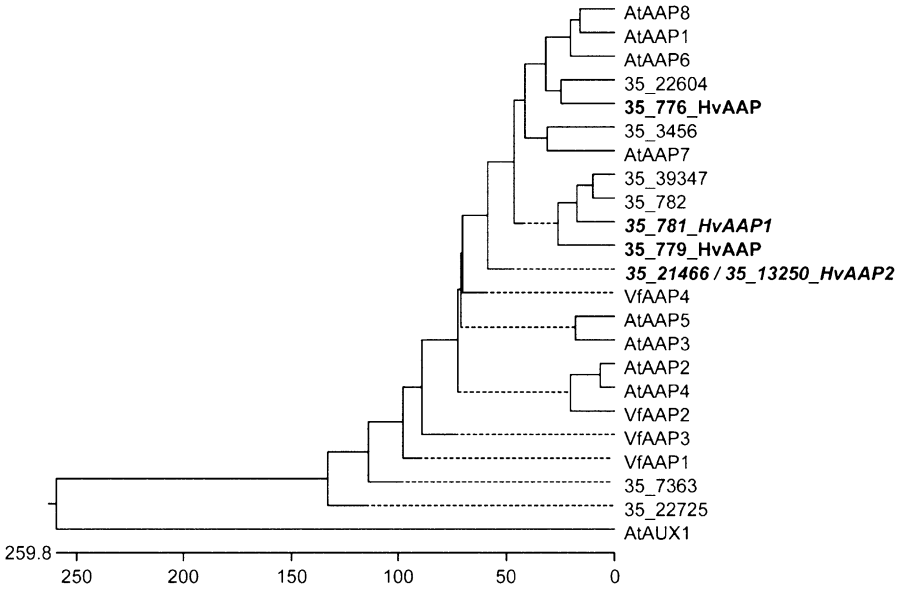

Figure 7. Dendrogram of amino acid permeases. Amino acid sequences were aligned using the ClustalW algorithm (DNA STAR). The order of branching within the dendrogram indicates similarities between putative amino acid permeases of barley and functionally characterized amino acid permeases of Arabidopsis and *V. faba*. For classification of amino acid permease sequences, assembly 35 of HarvEST: Barley (contains 444,652 ESTs) was used. Barley sequences are assigned according to the HarvEST unigene identifier. Up-regulated amino acid permeases in transfer cells (35_776 corresponds to clone HA16M17, 35_779 corresponds to clone HZ36G22) are given in boldface. Full-length HvAAP1 and HvAAP2 were characterized recently (C. Seiler, unpublished data) and are marked in boldface and italics. The scale at bottom indicates the distances between sequences. Accession numbers are as follows: AtAAP1, CAA47603; AtAAP2, CAC05448; AtAAP3, NP_177862; AtAAP4, BAB11033; AtAAP5, NP_175076; AtAAP6, CAA65051; AtAAP7, BAB10054; AtAAP8, AAC34329; VfAAP1, CAC51423; VfAAP2, CAA70778; VfAAP3, CAC51424; VfAAP4, CAC51425. The putative auxin carrier AUX1 from Arabidopsis (CAA67308) was used as an outgroup.

mildew fungi (P. Schweitzer, unpublished data). Subsequently, up-regulated proteolytic functions in ETC might be related to the activation of defense mechanisms. This speculation is strengthened by high expression of the ethylene-induced Cys protease Mir1 (Fig. 6), which mediates resistance against insects (Harfouche et al., 2006). Antifungal activity was also shown for basal layer antifungal proteins, expressed in the basal ETC layer of maize kernels (Serna et al., 2001). The possibility of the activation of defense mechanisms is further supported by transcriptional up-regulation of GDP-D-Man pyrophosphorylase (Table VI). The enzyme is rate limiting for ascorbate biosynthesis, a compound well-known as a reactive oxygen species scavenger.

Ethylene metabolism is transcriptionally stimulated in ETC, indicated by up-regulated expression of transcripts encoding enzymes of ethylene biosynthesis and catabolism. Expression of *Mir-CP* and a group of *AP2/EREPB*-like transcription factors (Table IV) points to the activation of gene expression by ethylene. Arabidopsis AP2 has a regulating role for the establishment of the flower meristem and flower organ identity (Jofuku et al., 2005) but may also be important for controlling seed size and weight and storage compound accumulation (Jofuku et al., 2005; Ohto et al., 2005). The AP2 influence was described as being of maternal origin (Ohto et al., 2005). However, reciprocal crosses combining the recessive *ap2-10* mutant allele to the *AP2* wild type showed clear influences of the endosperm-mediated *AP2* gene dosage effect on seed traits (Jofuku et al., 2005). Although somewhat speculative at the moment, the ethylene-mediated response in ETC might significantly influence barley grain development, as postulated for Arabidopsis.

Cell Wall Biosynthesis Differs between NP and ETC and Is Controlled by TPS/TPP

NP cells show wall thickening and invaginations in accordance with the formation of transport-active surfaces (Weschke et al., 2000). This is in agreement with the up-regulation of genes involved in cellulose synthesis, such as Suc synthases 1 and 2 and cellulose synthase 4. The product of Suc synthase, UDP-Glc, is the precursor for cellulose formation. Its oxidation via UDP-D-Glc dehydrogenase and the microsomal UDP-Glc decarboxylase (up-regulated in NP) yields UDP-Xyl, the glycosyl donor for arabinoxylans and arabinogalactan protein biosynthesis (Reiter and Vanzin, 2001).

In ETC, the concerted action of UDP-Glc pyrophosphorylase, phosphomannomutase, and GPD-Man pyrophosphorylase may provide activated D-Man, which is used by mannan synthases for the synthesis of

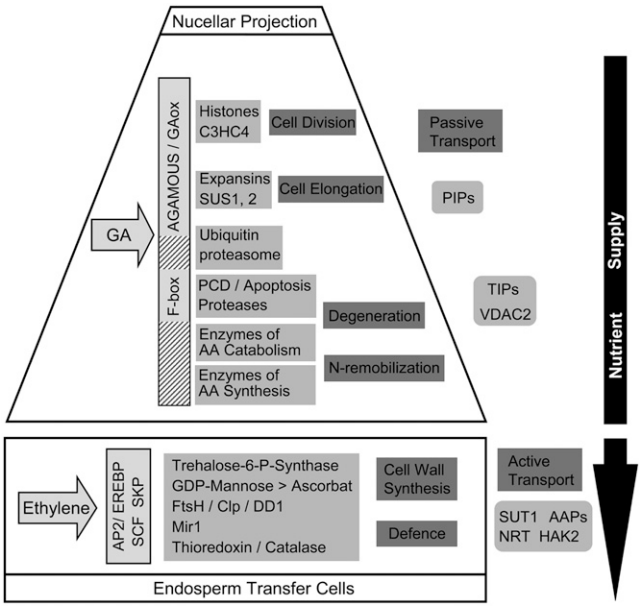

Figure 8. Model of cellular processes in NP and ETC at 8 DAF as deduced from transcriptome analysis. Further explanations are given in the text.

N-linked glycans and Man-containing cell wall components, such as glucomannans and galactomannans (Reiter and Vanzin, 2001). However, GDP-D-Man is also rate limiting for L-ascorbate biosynthesis (Smirnoff and Wheeler, 2000). Repression of *GDP-D-mannose pyrophosphorylase* in potato (*Solanum tuberosum*) leaves caused significant reductions in cell wall Man and L-ascorbate content (Keller et al., 1999). Interestingly, potato antisense lines show an early senescence phenotype possibly caused by oxidative damage. In this context, it has to be remarked that ETC (and aleurone transfer cells) form the only persisting tissue in the barley endosperm not undergoing PCD. Thus, an increased production of ascorbate as well as congruent higher expression of catalase and redox-related genes in ETC (HB07G07, HB29N12, HA04I24, and HA25P20; Supplemental Table S3) could improve resistance against oxidative damage and, thereby, avoid senescence.

Apart from its role in assimilate uptake, ETC walls also define cell and organ shape, act as barriers against the maternal pericarp, and possibly provide signals directing endosperm growth and development. An ordered deposition of cell wall material determines the shape of cells and organs (Zhong and Ye, 2007) and may require coordination of carbon partitioning between primary metabolism and cell wall synthesis. *TPS/TPP*s are strongly up-regulated in ETC. TPS/TPPs are shown to be major regulators of plant carbon metabolism (Paul et al., 2008). Arabidopsis cell walls of *tps1* embryos have altered structure and composition. In particular, genes involved in sugar nucleotide and pectin metabolism are altered (Gomez et al., 2006). Among the 20 cell wall-related transcripts found to be down-regulated in the *tps1* cells (Gomez et al., 2006), six genes show homology to transcripts up-regulated in barley ETC (two pectinesterases, mannosidase, glucosidase, expansin, and extensin). It can be speculated that TPS/TPPs play a regulatory role in the turnover of cell wall components and/or pectins in barley ETC. The Arabidopsis *cell shape phenotype1* mutation dramatically affected leaf epidermis, with loss of pavement cell lobes, altered morphology of trichomes, and different developmental alterations. The mutation was found in *AtTPS6*, encoding a class II TPS/TPP enzyme (Chary et al., 2008). Notably, up-regulated *TPS/TPP*s in ETC belong to the class II type, underlining its important role in the coordination of sugar partitioning, cell wall synthesis, and organ shape.

In this study, we analyzed differences in the transcriptome of NP and ETC in barley grains at 8 DAF. Regulatory networks of cellular differentiation and function seem to be coordinated by hormones, namely GAs in NP and ethylene in ETC. Hormonal regulation in both tissues undergoes fine-tuning, as concluded from the parallel transcriptional activation of biosynthesis and catabolism. However, cellular localization of the two antagonistic pathways is unknown. LMPC-based separation of the different NP regions coupled to transcriptome analysis would be helpful to address this question. Another feature of high interest is cell wall thickening in the lower part of NP and comparison with processes that establish transfer cell morphology in ETC. In ETC, cell wall metabolism seems to be controlled by trehalose-6-P signaling, possibly coupled to ethylene action.

Our interest was focused only on candidate genes that are differentially expressed between the two tissues. Consequently, potentially interesting similar regulatory/signaling processes that may exist in both tissues are missing. LMPC-coupled expression profiling of a time series of NP and ETC development could answer the question for both different and similar regulatory programs in either NP or ETC in relation to barley grain development.

MATERIALS AND METHODS

Plant Material

Barley (*Hordeum vulgare* 'Barke') was grown in greenhouses at 18°C with 16 h of light and humidity of 60%. Flowers are tagged as described by Weschke et al. (2000), and caryopses were harvested at 8 DAF.

Tissue Preparation for Microdissection

Caryopses were divided into thirds and fixed for 12 to 24 h at 4°C in 3:1 (v/v) ethanol-acetic acid (Farmer's fixative), formaldehyde-acetic acid-ethanol, or 3:1 (v/v) ethanol-water. Fixatives were infiltrated into segments under vacuum, 15 min on ice, and repeated three times. After fixation, tissue was dehydrated in a graded series of ethanol and infiltrated with increasing concentrations of Steedman's wax at 40°C (a polyester with low-melting-point polyethyleneglycol-distearate in 1-hexadecanol [9:1, w/w]; Vitha et al., 1997). Sections (20 μm) were prepared using a rotary microtome (Leica RM 2165), floated on water and mounted to PEN membrane slides (PALM), air dried,

and stored at 4°C in sealed slide boxes. Prior to microdissection, Steedman's wax was removed by incubating slides in an ethanol series from 30% to 100%. To evaluate the influence of fixation on RNA quality, completely sectioned caryopses were dewaxed in a graded ethanol series, air dried, and homogenized with mortar and pestle. A small proportion of the mixture was used for RNA extraction (see below).

LMPC

The PALM Laser Microbeam instrument was used to dissect distinct tissues from dewaxed, dried cross sections. The power of the laser beam (diameter <1.0 μm) was adjusted to 45 to 60 mW for cutting and to 70 to 90 mW for laser pressure catapulting. PALM RoboSoftware was used as a graphic tool for targeting of cells. Sections from NP and transfer cells were catapulted into the lid of 0.5-mL PALM Adhesive Caps. Typically, between 12 and 25 sections were processed per cap. Sections from two tubes were pooled prior to RNA isolation. The efficiency of tissue transfer to reaction tubes was optically controlled by microscope. The number of cells was estimated by cell counting using stained sections and multiplication of calculated cell layers and number of sections.

RNA Extraction and RNA Amplification

RNA was extracted from microdissected cells using the Absolutely RNA Nanoprep Kit (Stratagene) with slight modifications. After centrifugation (5 min, 13,000 rpm) to spin down sections, samples were vortexed (2 min) and incubated in lysis buffer (60°C, 5 min) containing 0.7% (v/v) β-mercaptoethanol. After lid abscission, the lid of the second cap with the corresponding sample was put on the reaction cup and processed in the same manner. RNA was treated with RNAse-free DNase I on a fiber matrix column and eluted with 10 μL of prewarmed elution buffer, yield was determined using NanoDrop (Ambion), and RNA quality was analyzed by microcapillary electrophoresis on the Experion automated electrophoresis system using the Experion RNA HighSens Analysis Kit (Bio-Rad Laboratories). T7 RNA polymerase-based RNA amplification was performed using the MessageAmp aRNA Kit (Ambion). Probes were labeled with [^{33}P]UTP during the second round of amplification to generate phosphorylated aRNA. After purification, labeled probes were denatured (5 min, 70°C) and cooled on ice (5 min) before hybridization. Reference probes for fidelity check of RNA amplification and tissue fixation were prepared according to Sreenivasulu et al. (2002). Purified total RNA (35 μg) from shock-frozen caryopses of the same developmental stage was used to synthesize [^{33}P]CTP-labeled cDNA probes.

cDNA Macroarray Analysis

The 12K barley seed array was hybridized and processed after Sreenivasulu et al. (2006), exposed to phosphor image screens for 20 h, and scanned at 100-μm resolution using a Fuji BAS 3000 phosphor scanner.

Data Analysis

Images of hybridized nylon membranes were subjected to automatic spot detection using a suite of customized MATLAB programs. The total number of 11,786 genes per array is covered by 23,572 double spots, enabling one technical replicate per gene for quality control. Additionally, we also considered gene expression levels from independently grown samples to check biological reproducibility. These combinations resulted in two technical and two biological data sets. Quantile normalization was carried out on the complete data set (Bolstad et al., 2003). During further analysis, genes with marginal expression values or diverging double spot ratios were eliminated. Fold changes between NP and ETC were derived from averages of four individual fold changes over the two technical and two biological replicates. The differentially expressed genes with at least 3-fold difference were identified between NP and ETC and cross-checked for biological reproducibility. Gene sets were functionally annotated after Sreenivasulu et al. (2006).

Quantitative Real-Time PCR

Total RNA was extracted from microdissected cells (as described above) and reverse transcribed using the SuperScript III First-Strand Synthesis System for RT-PCR (Invitrogen). The Power SYBR Green PCR Mastermix was used to perform reactions in the ABI 7900 HT real-time PCR system (Applied Biosystems). Five replications were conducted for each of the selected genes. Expression values were normalized with transcript levels of an *actin1* gene (cn2343g02; consensus sequence from the IPK Crop EST Database) from barley and calculated as an arithmetic mean of the replicates. Dissociation curves confirmed the presence of a single amplicon in each PCR. Fold changes were calculated after Livak and Schmittgen (2001).

In Situ Hybridization

Barley caryopses were fixed in 4% (v/v) paraformaldehyde in phosphate-buffered saline, pH 7.3, overnight at 4°C. After dehydration through an ethanol series, samples were passed through a graded ethanol-methacrylate series after Baskin et al. (1992) and polymerized for at least 48 h in UV light (20°C). Cross sections (7 μm) were prepared and mounted to silane-coated slides (Sigma-Aldrich). Digoxigenin-labeled antisense and sense RNA were synthesized using T3 or T7 RNA polymerase (Roche). Hybridization and immunological detection was performed after Drea et al. (2005), and hybridization signals were detected by alkaline phosphatase-conjugated anti-digoxigenin antibody and visualized with 4-nitroblue tetrazolium chloride and 5-bromo-4-chloro-3-indolyl phosphate (Roche).

Light Microscopy

Cross sections (2 mm) of barley caryopses were fixed in 2.5% (v/v) glutaraldehyde and 2% (v/v) formaldehyde in 50 mM cacodylate buffer, pH 7.2, overnight at 4°C for primary fixation. After washing with 50 mM cacodylate buffer and water, a second fixation step with 1% (w/v) OsO_4 was performed. After 1 h of infiltration, samples were washed three times with water and embedded in resin. Resin embedding, sectioning, and staining for light microscopy was performed after Tognetti et al. (2006).

Sequence data from this article can be found at http://pgrc.ipk-gatersleben.de/cr-est/.

Supplemental Data

The following materials are available in the online version of this article.

Supplemental Table S1. Fidelity of gene expression levels in amplified probes with and without fixation treatment.

Supplemental Table S2. Differentially expressed genes involved in DNA synthesis with 3-fold or greater changes between NP and ETC.

Supplemental Table S3. List of differentially expressed genes between NP and ETC with annotation, normalized expression values, and calculated fold changes.

ACKNOWLEDGMENTS

We are grateful to Uta Siebert and Monika Wiesner for their excellent technical assistance and to Karin Lipfert for graphical artwork.

Received August 4, 2008; accepted September 5, 2008; published September 10, 2008.

LITERATURE CITED

Adrain C, Martin SJ (2001) The mitochondrial apoptosome: a killer unleashed by the cytochrome seas. Trends Biochem Sci **26:** 390–397

Alboresi A, Gestin C, Leydecker MT, Bedu M, Meyer C, Truonq HN (2005) Nitrate, a signal relieving seed dormancy in Arabidopsis. Plant Cell Environ **28:** 500–512

Baskin TI, Busby CH, Fowke LC, Sammut M, Gubler F (1992) Improvements in immunostaining samples embedded in methacrylate: localisation of microtubules and other antigens throughout developing organs in plants of diverse taxa. Planta **187:** 405–413

Becraft PW (1999) Development of the leaf epidermis. Curr Top Dev Biol **45:** 1–40

Beers EP, Woffenden BJ, Zhao C (2000) Plant proteolytic enzymes: possible roles during programmed cell death. Plant Mol Biol **44:** 399–415

Bolstad BM, Irizarry RA, Astrand M, Speed TP (2003) A comparison of normalization methods for high density oligonucleotide array data based on bias and variance. Bioinformatics **19:** 185–193

Borisjuk L, Wang TL, Rolletschek H, Wobus U, Weber H (2002) A pea seed mutant affected in the differentiation of the embryonic epidermis is impaired in embryo growth and seed maturation. Development **129:** 1595–1607

Burgemeister R, Gangnus R, Haar B, Schutze K, Sauer U (2003) High quality RNA retrieved from samples obtained by using LMPC (laser microdissection and pressure catapulting) technology. Pathol Res Pract **199:** 431–436

Cai S, Lashbrook CC (2006) Laser capture microdissection of plant cells from tape-transferred paraffin sections promotes recovery of structurally intact RNA for global gene profiling. Plant J **48:** 628–637

Casson S, Spencer M, Walker K, Lindsay K (2005) Laser capture microdissection for the analysis of gene expression during embryogenesis of Arabidopsis. Plant J **42:** 111–123

Chary SN, Hicks GR, Choi YG, Carter D, Raikhel NV (2008) Trehalose-6-phosphate synthase/phosphatase regulates cell shape and plant architecture in Arabidopsis. Plant Physiol **146:** 97–107

Chen F, Foolad MR (1997) Molecular organization of a gene in barley which encodes a protein similar to aspartic protease and its specific expression in nucellar cells during degeneration. Plant Mol Biol **35:** 821–831

Chen JM, Dando PM, Rawlings ND, Brown MA, Young NE, Stevens RA (1997) Cloning, isolation and characterization of mammalian legumain, an asparaginyl endopeptidase. J Biol Chem **272:** 8090–8098

Close TJ, Wanamaker S, Roose ML, Lyon M (2007) HarvEST: an EST database and viewing software. Methods Mol Biol **406:** 161–178

Coffeen WC, Wolpert TJ (2004) Purification and characterization of serine proteases that exhibit caspase-like activity and are associated with programmed cell death in *Avena sativa*. Plant Cell **16:** 857–873

Deiss LP, Galinka H, Berissi H, Cohen O, Kimchi A (1996) Cathepsin D protease mediates programmed cell death induced by interferon-gamma, Fas/APO-1 and TNF-alpha. EMBO J **15:** 3861–3870

Drea S, Leader DJ, Arnold BC, Shaw P, Dolan L, Doonan JH (2005) Systematic spatial analysis of gene expression during wheat caryopsis development. Plant Cell **17:** 2172–2185

Duggan DJ, Bittner M, Chen Y, Meltzer P, Trent JM (1999) Expression profiling using cDNA microarrays. Nat Genet **21:** 10–14

Elkeles A, Devos KM, Graur D, Zizi M, Breimann A (1995) Multiple cDNAs of wheat voltage-dependent anion channels (VDAC): isolation, differential expression, mapping and evolution. Plant Mol Biol **29:** 109–124

Emmert-Buck MR, Bonner RF, Smith PD, Chuaqui RF, Zhuang Z, Goldstein SR, Weiss RA, Liotta LA (1996) Laser capture microdissection. Science **274:** 998–1001

Fleury D, Himanen K, Cnops G, Nelissen H, Boccardi TM, Maere S, Beemster GT, Neyt P, Anami S, Robles P, et al (2007) The *Arabidopsis thaliana* homolog of yeast BRE1 has a function in cell cycle regulation during early leaf and root growth. Plant Cell **19:** 417–432

Gagne JM, Smalle J, Gingerich DJ, Walker JM, Yoo SD, Yanagisawa S, Viestra RD (2004) Arabidopsis EIN3-binding F-box1 and 2 form ubiquitin-protein ligases that repress ethylene action and promote growth by directing EIN3 degradation. Proc Natl Acad Sci USA **101:** 6803–6808

Goldbole A, Varghese J, Sarin A, Mathew MK (2003) VDAC is a conserved element of death pathways on plant and animal systems. Biochim Biophys Acta **1642:** 87–96

Gomez LD, Baud S, Gilday A, Li Y, Graham IA (2006) Delayed embryo development in the Arabidopsis *trehalose-6-phosphate synthase1* mutant is associated with altered cell wall structure, decreased cell division and starch accumulation. Plant J **46:** 69–84

Gomez-Mena C, de Folter S, Costa MMR, Angenent GC, Sablowski R (2004) Transcriptional program controlled by the floral homeotic gene AGAMOUS during early organogenesis. Development **132:** 429–438

Griffith EC, Hosken SE, Oliver D, Chojecki J, Thomas H (1997) Sequencing, expression pattern and RFLP mapping of a senescence-enhanced cDNA of *Zea mays* with homology to oryzain γ and aleurain. Plant Mol Biol **34:** 815–821

Guerrero C, de la Calle M, Reid MS, Valpuesta V (1998) Analysis of the expression of two thiolprotease genes from daylily (*Hemerocallis* ssp.) during flower senescence. Plant Mol Biol **36:** 565–571

Harfouche A, Shivaji R, Stocker R, Williams PW, Luthe DS (2006) Ethylene signalling mediates a maize defence response to insect herbivory. Mol Plant Microbe Interact **19:** 189–199

Hays DB, Yeung EC, Pharis RP (2002) The role of gibberellins in embryo axis development. J Exp Bot **53:** 1747–1751

Hirner B, Fischer WN, Rentsch D, Kwart M, Frommer WB (1998) Developmental control of H^+/amino acid permease gene expression during seed development of Arabidopsis. Plant J **14:** 535–544

Hueros G, Royo J, Maitz M, Salamini F, Thompson RD (1999) Evidence for factors regulating cell-specific expression in maize endosperm. Plant Mol Biol **41:** 403–414

Hunter PR, Craddock CP, Di Benedetto S, Roberts LM, Frigerio L (2007) Fluorescent reporter proteins for the tonoplast and the vacuolar lumen identify a single vacuolar compartment in Arabidopsis cells. Plant Physiol **145:** 1371–1382

Jauh GY, Fischer AM, Grimes HD, Ryan CA, Rogers JC (1998) Delta-tonoplast intrinsic protein defines unique plant vacuole functions. Proc Natl Acad Sci USA **95:** 12995–12999

Jauh GY, Phillips TE, Rogers JC (1999) Tonoplast intrinsic protein isoforms as markers for vacuolar functions. Plant Cell **11:** 1867–1882

Jofuku KD, Omidyar PK, Gee Z, Okamuro JK (2005) Control of seed mass and seed yield by the floral homeotic gene APETALA2. Proc Natl Acad Sci USA **102:** 3117–3122

Kanervo E, Singh M, Suorsa M, Paakkarinen V, Aro E, Battchikova N, Aro EM (2008) Expression of protein complexes and individual proteins upon transition of etioplasts to chloroplasts in pea (*Pisum sativum*). Plant Cell Physiol **49:** 396–410

Keller R, Renz FS, Kossmann J (1999) Antisense inhibition of the GDP-mannose pyrophosphorylase reduces the ascorbate content in transgenic plants leading to developmental changes during senescence. Plant J **19:** 131–141

Laux T, Jürgens G (1997) Embryogenesis: a new start in life. Plant Cell **9:** 989–1000

Linnestad C, Doan DN, Brown RC, Lemmon BE, Meyer DJ, Jung R, Olsen OA (1998) Nucellain, a barley homolog of the dicot vacuolar-processing protease, is localized in nucellar cell walls. Plant Physiol **118:** 1169–1180

Liu Y, Koornneef M, Soppe WJ (2007) The absence of histone H2B monoubiquitination in the Arabidopsis *hub1* (*rdo4*) mutant reveals a role for chromatin remodelling in seed dormancy. Plant Cell **19:** 433–444

Livak KJ, Schmittgen TD (2001) Analysis of relative gene expression data using real-time quantitative PCR and the $2^{-\Delta\Delta CT}$ method. Methods **25:** 402–408

Lombardi L, Casani S, Ceccarelli N, Galleschi L, Picciarelli P, Lorenzi R (2007) Programmed cell death of the nucellus during *Sechium edule* Sw. seed development is associated with activation of caspase-like proteases. J Exp Bot **58:** 2949–2958

Luo L, Salunga RC, Guo H, Bittner A, Joy KC, Galindo JE, Xiao H, Rogers KE, Wan JS, Jackson MR, et al (1999) Gene expression profiles of laser-captured adjacent neuronal subtypes. Nat Med **5:** 117–122

Nakazano M, Qiu F, Borsuk LA, Schnable PS (2003) Laser-capture microdissection, a tool for the global analysis of gene expression in specific plant cell types: identification of genes expressed differentially in epidermal cells or vascular tissues of maize. Plant Cell **15:** 583–596

Noh YS, Amasino RM (1999) Regulation of developmental senescence is conserved between Arabidopsis and *Brassica napus*. Plant Mol Biol **41:** 195–206

Nygaard V, Hovig E (2006) Options available for profiling small samples: a review of sample amplification technology when combined with microarray profiling. Nucleic Acids Res **34:** 996–1014

Offler CE, McCurdy DW, Patrick JW, Talbot MJ (2002) Transfer cells: cells specialized for a special purpose. Annu Rev Plant Biol **54:** 431–454

Ohto M, Fischer RL, Goldberg RB, Nakamura K, Harada JJ (2005) Control of seed mass by APETALA2. Proc Natl Acad Sci USA **102:** 3123–3128

Ohtsu K, Smith MB, Emrich SJ, Borsuk LA, Zhou R, Chen T, Zhang X, Timmermanns MCP, Beck J, Janick-Bruckner D, et al (2007) Global gene expression analysis of the shoot apical meristem of maize (*Zea mays* L.). Plant J **52:** 391–404

Okumoto S, Schmidt R, Tegeder M, Fischer WN, Rentsch D, Frommer WB, Koch W (2002) High affinity amino acid transporters specifically expressed in xylem parenchyma and developing seeds of Arabidopsis. J Biol Chem **277:** 45338–45346

Olsen OA (2001) Endosperm development: cellularization and cell fate specification. Annu Rev Plant Physiol Plant Mol Biol **52:** 233–267

Olsen OA (2004) Nuclear endosperm development in cereals and *Arabidopsis thaliana*. Plant Cell (Suppl) **16:** S214–S227

Olsen OA (2007) Endosperm: Developmental and Molecular Biology. Springer Verlag, Berlin

Ostersetzer O, Adam Z (1997) Light-stimulated degradation of an unassembled Rieske FeS protein by a thylakoid-bound protease: the possible role of the FtsH protease. Plant Cell **9:** 957–965

Otegui MS, Noh YS, Martinez DE, Petroff MGV, Staehelin LA, Amasino RM, Guiamet JJ (2005) Senescence-associated vacuoles with intense proteolytic activity develop in leaves of Arabidopsis and soybean. Plant J **41:** 831–844

Patrick JW, Offler CE (1995) Post-sieve element transport of sucrose in developing seed. Aust J Plant Physiol **22:** 681–702

Patrick JW, Offler CE (2001) Compartmentation of transport and transfer events in developing seeds. J Exp Bot **52:** 551–564

Paul MJ, Primavesi LF, Jhurreea D, Zhang Y (2008) Trehalose metabolism and signalling. Annu Rev Plant Biol **59:** 417–441

Pereira LA, Schoor S, Goubet F, Dupree P, Moffatt BA (2006) Deficiency of adenosine kinase activity affects the degree of pectin methyl-esterification in cell walls of *Arabidopsis thaliana*. Planta **224:** 1401–1414

Radchuk V, Borisjuk L, Radchuk R, Steinbiss HH, Rolletschek H, Broeders S, Wobus U (2006) Jekyll encodes a novel protein involved in the sexual reproduction of barley. Plant Cell **18:** 1652–1666

Rawlings ND, Barrett AJ (1994) Families of cysteine peptidases. Methods Enzymol **244:** 461–486

Reape TJ, Molony EM, McCabe PF (2008) Programmed cell death in plants: distinguishing between different modes. J Exp Bot **59:** 435–444

Reiter WD, Vanzin GF (2001) Molecular genetics of nucleotide sugar interconversion pathways in plants. Plant Mol Biol **47:** 95–113

Richmond T, Somerville S (2000) Chasing the dream: plant EST microarrays. Curr Opin Plant Biol **3:** 108–116

Runeberg-Roos P, Törmäkangas K, Östman A (1991) Primary structure of a barley-grain aspartic proteinase: a plant aspartic proteinase resembling cathepsin D. Eur J Biochem **202:** 1021–1027

Sakamoto T, Kobayashi M, Itoh H, Tagiri A, Kayano T, Tanaka H, Iwahori S, Matsuoka M (2001) Expression of a gibberellin 2-oxidase gene around the shoot apex is related to phase transition in rice. Plant Physiol **125:** 1508–1516

Scott DB, Jin W, Ledford HK, Jung HS, Honma MA (1999) EAF1 regulates vegetative-phase change and flowering time in Arabidopsis. Plant Physiol **120:** 675–684

Senn ME, Rubio F, Banuelos MA, Rodriguez-Navarro A (2001) Comparative functional features of plant potassium HvHAK1 and HvHAK2 transporters. J Biol Chem **276:** 44563–44569

Serna A, Maitz M, O'Connell T, Santandrea G, Thevissen K, Hueros G, Faleri C, Cai G, Lottspeich F, Thompson RD (2001) Maize endosperm secretes a novel antifungal protein into adjacent maternal tissue. Plant J **25:** 687–698

Shindo T, Van der Hoorn RAL (2008) Papain-like cysteine proteases: key players at molecular battlefields employed by both plants and their invaders. Mol Plant Pathol **9:** 119–125

Smirnoff N, Wheeler GL (2000) Ascorbic acids in plants: biosynthesis and function. Crit Rev Biochem Mol Biol **35:** 291–314

Spencer MWB, Casson SA, Lindsey K (2006) Transcriptional profiling of the Arabidopsis embryo. Plant Physiol **143:** 924–940

Sreenivasulu N, Altschmied L, Panitz R, Hähnel U, Michalek W, Weschke W, Wobus U (2002) Identification of genes specifically expressed in maternal and filial tissues of barley caryopsis: a cDNA array analysis. Mol Genet Genomics **266:** 758–767

Sreenivasulu N, Altschmied L, Radchuk V, Gubatz S, Wobus U, Weschke W (2004) Transcript profiles and deduced changes of metabolic pathways in maternal and filial tissues of developing barley grains. Plant J **37:** 539–553

Sreenivasulu N, Radchuk V, Strickert M, Miersch O, Weschke W, Wobus U (2006) Gene expression patterns reveal tissue-specific signaling networks controlling programmed cell death and ABA-regulated maturation in developing barley seeds. Plant J **47:** 310–327

Sreenivasulu N, Usadel B, Winter A, Radchuk V, Scholz U, Stein N, Weschke W, Strickert M, Close TJ, Stitt M, et al (2008) Barley grain maturation and germination: metabolic pathways and regulatory network commonalities and differences highlighted by new MapMan/PageMan profiling tools. Plant Physiol **146:** 1738–1758

Stone S, Callis J (2007) Ubiquitin ligases mediate growth and development by promoting protein death. Curr Opin Plant Biol **10:** 624–632

Sun TP, Gubler F (2004) Molecular mechanism of gibberellin signalling. Annu Rev Plant Biol **55:** 197–223

Sun X, Peng L, Guo J, Chi W, Ma J, Lu C, Zhang L (2007) Formation of DEG5 and DEG8 complexes and their involvement in the degradation of photodamaged photosystem II reaction center D1 protein in *Arabidopsis*. Plant Cell **19:** 1347–1361

Thompson RD, Hueros G, Becker H, Maitz M (2001) Development and function of seed transfer cells. Plant Sci **160:** 775–783

Tognetti VB, Palatnik JF, Fillat MF, Melzer M, Hajirezaei M, Valle EM, Carillo N (2006) Functional replacement of ferredoxin by a cyanobacterial flavodoxin in tobacco confers broad-range stress tolerance. Plant Cell **18:** 2035–2050

Tsujimoto Y, Shimizu S (2002) The voltage-dependent anion channel: an essential player in apoptosis. Biochimie **84:** 187–193

Vierstra RD (2003) The ubiquitin/26S proteasome pathway, the complex last chapter in the life of many plant proteins. Trends Plant Sci **8:** 135–142

Vitha S, Baluska F, Mews M, Volkman D (1997) Immunofluorescence detection of F-actin on low melting point wax sections from plant tissues. J Histochem Cytochem **45:** 89–95

Wang H, Caruso LV, Downie AB, Perry SE (2004) The embryo MADS domain protein Agamous-like 15 directly regulates expression of a gene encoding an enzyme involved in gibberellin metabolism. Plant Cell **16:** 1206–1219

Weber H, Borisjuk L, Wobus U (2005) Molecular physiology of legume seed development. Annu Rev Plant Biol **56:** 253–279

Weschke W, Panitz R, Gubatz S, Wang Q, Radchuk R, Weber H, Wobus U (2003) The role of invertases and hexose transporters in controlling sugar ratios in maternal and filial tissues of barley caryopses during early development. Plant J **33:** 395–411

Weschke W, Panitz R, Sauer N, Wang Q, Neubohn B, Weber H, Wobus U (2000) Sucrose transport into developing barley seeds: molecular characterization of two transporters and implications for seed development and starch accumulation. Plant J **21:** 455–467

Wheeler D, Newbigin E (2007) Expression of 10 S-class SLF-like genes in *Nicotiana alata* pollen and its implications for understanding the pollen factor of the S locus. Genetics **177:** 2171–2180

Williams J, Phillips AL, Gaskin P, Hedden P (1998) Function and substrate specificity of the gibberellin 3-beta-hydroxylase encoded by the Arabidopsis *GA4* gene. Plant Physiol **117:** 559–563

Woll K, Borsuk LA, Stransky H, Nettleton D, Schnable PS, Hochholdinger F (2005) Isolation, characterization, and pericycle-specific transcriptome analysis of the novel maize lateral and seminal root initiation mutant *rum1*. Plant Physiol **139:** 1255–1267

Xu FX, Chye ML (1999) Expression of cysteine proteinase during developmental events associated with programmed cell death. Plant J **17:** 321–327

Young TE, Gallie DR (2000) Programmed cell death during endosperm development. Plant Mol Biol **44:** 283–301

Zhang WH, Zhou Y, Dibley KE, Tyerman SD, Furbank RT, Patrick JW (2007) Nutrient loading of developing seeds. Funct Plant Biol **34:** 314–331

Zhong R, Ye ZH (2007) Regulation of cell wall biosynthesis. Curr Opin Plant Biol **10:** 564–572